Atomic structure and orientation relations of interfaces between Ag and ZnO

Vellinga, W.P; de Hosson, J.T.M.

Published in:
Acta Materialia

DOI:
10.1016/S1359-6454(96)00252-2

Pergamon

PII: S1359-6454(96)00252-2

Acta mater. Vol. 45, No. 3, pp. 933–950, 1997

Published by Elsevier Science Ltd

1359-6454/97 $17.00 + 0.00

ATOMIC STRUCTURE AND ORIENTATION RELATIONS OF INTERFACES BETWEEN Ag AND ZnO

W. P. VELLINGA and J. TH. M. DE HOSSON†

Department of Applied Physics, Materials Science Center, University of Groningen, Nijenborgh 4, 9747 AG, Groningen, the Netherlands

(Received 10 January 1996; accepted 1 July 1996)

Abstract—This paper presents the results of investigations of Ag-ZnO interfaces, produced by internal oxidation of an Ag-Zn alloy. ZnO precipitates with the wurtzite structure were found exhibiting mainly one orientation relation with the Ag matrix. However, closely related ORs were found, rotated by small angles from that orientation relation. The atomic structures of several interfaces surrounding these precipitates were studied and compared using HRTEM. The paper concentrates on interfaces between low index facets of ZnO and vicinal planes of Ag. These interfaces clearly show relaxations. An interpretation of these relaxations in terms of dissociation of partial dislocations at the interface is put forward. *Copyright © 1997 Acta Metallurgica Inc.*

1. INTRODUCTION

With the advent of ultra-high resolution transmission electron microscopy (HRTEM) the atomic structure of many metal–ceramic interfaces has been investigated in recent years. Among the issues addressed using this technique were the chemical composition, translational state, and the degree of coherency of interfaces. For a recent review of these and other results on metal–ceramic interfaces we refer to [1]. Our interest lies with the latter issue and, more specifically, with the core structure of (misfit) dislocations near metal–ceramic interfaces. We combine HRTEM observations to reveal the structural features with a numerical model to interpret them. Although the model description embraces a rather strongly simplified picture of the oxide and of the interactions across the interface, it does allow us to study the effect of misfit and bond strength on the dislocation cores at or near the interface. The model was first employed by Vitek *et al.* to account for relaxations near a Nb-Al_2O_3 interface [2] and was extended by us [3, 4] to clarify the structure of the misfit dislocation network at a Cu-MgO interface and to compare the model with a description based on anisotropic linear elasticity of an array of misfit dislocations.

A relatively simple means of creating metal–oxide interfaces suited for HRTEM work is internal oxidation. It leads to the formation of oxide precipitates with a few orientation relations with the metal matrix. Orientation relations and interfaces that form cannot, in general, be predicted from the crystal structures of oxide and metal. It may even be impossible to predict beforehand which oxide will form. The presence of a metastable phase of ZnO in the samples we studied is a case in point here. The internal oxidation of alloys containing zinc has not received a lot of attention. From our point of view it seems to be an attractive choice for a number of reasons. First, the oxide expected to form is hexagonal. A precipitate will therefore necessarily show interfaces of rather different character. Moreover, precipitates of ZnO are expected to attain appreciable dimensions in several metals, owing to the rather low oxygen affinity of zinc. A comparison of interfaces formed in different metals therefore seems to be possible. This paper will concentrate on the interfaces between Ag and ZnO, and sometimes refer to the other data when necessary.

We did not study the influence of the oxidation parameters on the number, size, orientation and shape of the precipitates, because the size and faceting of the precipitates made them suitable for our goal: HRTEM observation of their interfaces. We are aware that, in particular, our lack of knowledge of the influence on precipitate shape and orientation at this point of time constrains the scope of our interpretations. In internal reduction, for example, dependence of the shape and orientation relation of precipitates on temperature has been shown [5], and recent investigations in our own laboratory indicate a similar fact for the internal oxidation of Cu-Mg alloys [6].

In literature studies of the internal oxidation of Zn in Cu, Ag and Pd are reported. Only the latter combination was also studied using (HR)TEM [7, 8]. Meijering reports that in Ag with 2 at% Zn, no "microscopically visible" precipitates of ZnO are formed, as opposed to ZnO in Cu [9]. This is in

†To whom all correspondence should be addressed.

agreement with the fact that precipitates tend to get larger if the difference in oxide affinity between the matrix and alloying element decreases. Our experiments confirm this tendency as precipitates of ZnO in Cu are somewhat larger than those of ZnO in Ag. In our case, a typical ZnO precipitate in Ag would indeed be just below the limit of what is visible in optical microscopy. Of all precipitates we came across, the majority had formed in the interior regions of grains, and were plate-like, with a thickness of the order of 100 nm and a diameter of the order of 1000 nm. They exhibit an orientation relation with the Ag matrix that will be referred to as OR1 hereafter and that is treated more thoroughly in Sections 4.1 and 4.2. In this OR the (polar) basal plane of the ZnO is parallel to a {111} plane in the Ag matrix. This OR has also been found for ZnO precipitates in Cu and Pd [7, 8, 10]. Three closely related ORs, rotated by a small angle with respect to OR1, have been encountered. These orientation relations were, however, very rare in our sample and were measured for one precipitate only. These are discussed in Sections 4.1 and 4.2 as well. Heterogeneously nucleated precipitates on grain boundaries also occur. Although they clearly do show facets, none of these precipitates ever did show one of the ORs that was found for the precipitates inside the grains. Surprisingly, some precipitates of ZnO were found that apparently had the sphalerite structure. This is a metastable phase of ZnO. Precipitates with this structure were rare and always found in contact with the wurtzite form. Questions regarding the nucleation and stability of this metastable phase are addressed in Section 5.

2. RELEVANT PROPERTIES OF ZnO

2.1. *Structural features*

At room temperature zinc-oxide, ZnO, generally occurs in the hexagonal wurtzite structure. The space group is $P6_3mc$. The JCPDS file for ZnO gives lattice parameters $a = 0.32482(9)$ nm, and $c = 0.520661(15)$ nm, at approximately 299 K [11]. A third parameter, u, is necessary to describe the structure. It is the distance, normalized with respect to c, along the c-axis between oxygen and zinc ions. The publications on which the JCPDS files are based give values of 0.3825(14) and 0.3826(7) for u [12, 13]. More recent neutron diffraction data give the following values: $a = 0.32501(1)$ nm, $c = 0.52701(1)$ nm, $u = 0.3817(1)$ [14]. A value of 3/8 for the parameter u would lead to a perfect tetrahedral arrangement of the atoms, but the deformation of the tetrahedra is small. The Zn-O distances along the c-axis are slightly (about 0.0019 nm) longer than along the other directions. The c/a ratio for ZnO is 1.6021, which can also be taken as a sign of slightly distorted tetrahedrons. ZnO is, however, polymorphic, and is also known to exist in two cubic structures. A high-pressure NaCl-like structure is metastable at atmospheric pressure at room temperature. The lattice parameter of this compound is 0.4280 nm [15].

ZnO also exists in a metastable sphalerite structure. The wurtzite and sphalerite arrangements are very much alike. The sphalerite structure is related to the wurtzite structure as cubic close packing is to hexagonal close packing. Both structures might be considered as composed of ZnO_4 tetrahedra. In the wurtzite structure these are stacked in a hexagonal close packed array with the tetrahedral edges of alternate layers rotated by 180°. In the sphalerite structure they are parallel in the layers that are repeated in a way so as to achieve cubic close-packing. Alternatively one could say that the sphalerite structure can be derived from f.c.c., and the wurtzite structure from h.c.p. by filling exactly half the tetrahedral holes in a regular manner with a second type of atom. As far as nearest neighbours are concerned, sphalerite and wurtzite are the same, each atom being surrounded by atoms of the other kind placed at the corners of a tetrahedron. Differences only become apparent if we look at next-nearest neighbours. Interactions between like atoms, Zn-Zn or O-O, are less important in the wurtzite structure. This is also reflected in the Madelung constant of the two structures, being 1.638 for the sphalerite structure and 1.641 for the wurtzite structure. These values, although differing by only a small amount, suggest that the wurtzite structure is somewhat more favourable for ionic compounds and the sphalerite structure for covalent compounds. The structures being so alike, no important differences in energy are expected to exist between them. Indeed *ab initio* total energy calculations show the energy of the sphalerite phase to be higher by only about 0.05 eV per formula unit [16]. Nevertheless, polytypism and stacking disorder in ZnO are not common, whereas ZnS, for example, is notorious for the amount of polytypes in which it crystallizes, and for the ease with which the stacking of close packed layers along the c-axis becomes disordered.

To the best of our knowledge the sphalerite form of ZnO has only been reported on two occasions, by Bragg *et al.* in 1932, and by Radczewski *et al.* in 1969 [17–19]. Bragg *et al.* found thin films of transparent ZnO spanning small holes in a Zn film. Electron diffraction patterns could be indexed for a cubic structure, and the intensities measured indicated a sphalerite form. The lattice constant was estimated to be 0.462 nm. Radczewski *et al.* studied ZnO scales on Zn particles. Electron diffraction patterns of thin filaments were interpreted by assuming a cubic form of ZnO to be present, with a lattice parameter of 0.5587 nm. This seems to be incorrect for ZnO with a sphalerite structure. It would mean an elongation of the Zn-O bonds compared with their length in hexagonal ZnO, by about 21%, which is rather unlikely. The possibility that a different compound is responsible for these

measurements should not be disregarded. The basal plane is a polar surface, and may have metallic character. Ag deposited on these surfaces has been shown to grow in a layer by layer fashion, with a preferential orientation of the {111} plane of the individual Ag crystallites parallel to the surface, but without any strong azimuthal orientation of the crystallites [20]. An unreconstructed surface shows a hexagonal net of atomic rows with edges of 0.325 nm. This distance is larger than the nearest neighbour distance in most f.c.c. metals. If the layer below this also affects the bonding, the symmetry at the interface will be threefold. The $\langle 10\bar{1}0 \rangle$ plane, or first-order prism plane of ZnO is a non-polar surface. Several metals have been deposited on these surfaces, to study bonding. Au is reported to have a low interaction with this surface whereas the stability of Cu on $(10\bar{1}0)$ planes is intermediate between Cu on (0001) and $(000\bar{1})$.

3. EXPERIMENTAL DETAILS

A silver–zinc alloy was made containing 1 wt% of Zn. The Ag used was 99.995% pure and the Zn 99.9995%. Melting and subsequent cooling of the AgZn mixture was performed in a graphite crucible in an evacuated quartz tube. The samples were not homogenized after this treatment. Flakes of about 1 mm thickness were internally oxidized at 1073 K, in air. The oxidation time was quite long, 17 hours, and even three days for some samples. TEM specimen preparation was straightforward using standard preparation techniques. Specimens were ground, dimpled and ion-milled to electron transparency. Ion milling was performed with a GATAN dual ion mill. The accelerating voltage was 5 kV, and the milling angle 15°. HRTEM images were taken with a JEM4000//EX II microscope, operating at 400 kV. The relevant electron optical parameters of this microscope have been determined: $C_s = 0.97 \pm 0.02$ nm, defocus spread: 11 ± 2 nm, beam semi-convergence angle: 0.55 mrad.

HRTEM negatives were digitized, and the grey scale adapted to achieve a reasonable contrast. Of the images presented here only those in Figs 9 and 12(b) have been explicitly low-pass filtered to reduce noise.

4. RESULTS

4.1. Orientation relations

The predominant orientation relation, OR1 shows a parallelism of {0002} of ZnO with {111} of Ag, and $\langle 2\bar{1}\bar{1}0 \rangle$ of ZnO and $\langle 110 \rangle$ of Ag. This means there are four sets of equivalent precipitates, with this OR, each with their basal plane aligned to one of the four {111} planes. Viewed along any particular $\langle 110 \rangle$ direction, for two of these sets the basal plane is inclined to the beam, in the other two it is parallel to the beam. The orientation of the latter precipitates is mirror symmetric with respect to the {002} plane, which is parallel to that viewing direction. The same orientation relation has been found for ZnO precipitates in Cu and Pd.

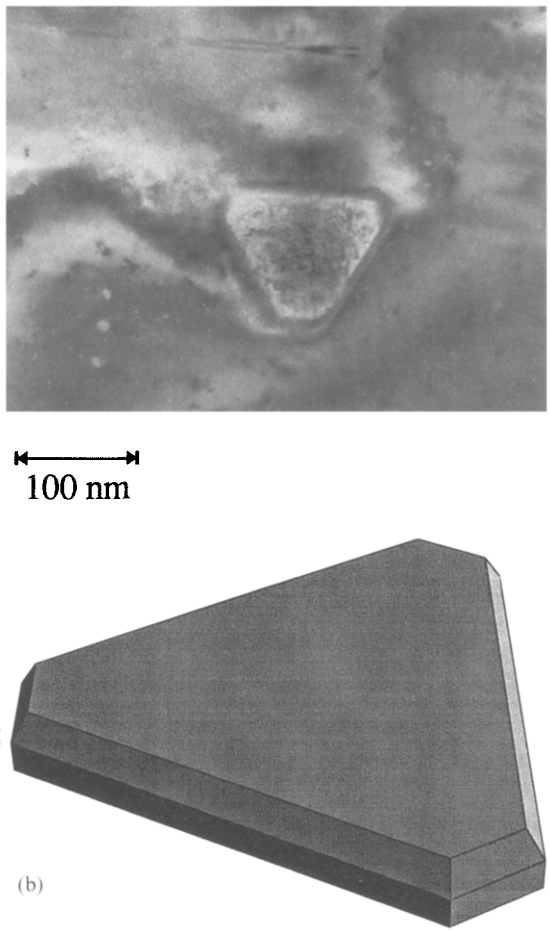

Fig. 1. (a) Precipitate of wurtzite ZnO, showing truncated trigonal shape. This is a rather small precipitate. View along $\langle 111 \rangle$, the edges are along $\langle 110 \rangle$ directions of the Ag. (b) Impression of the precipitates, showing basal plane, first-order pyramidal plane and first-order prismatic plane facets.

Viewing along a $\langle 111 \rangle$ axis, Fig. 1, it becomes clear that these precipitates have a truncated trigonal shape, dictated by the threefold axis of f.c.c. Ag around $\langle 111 \rangle$ directions. It is evident that the edges of the precipitate, as cut by the foil perpendicular to a $\langle 110 \rangle$ viewing direction, are not necessarily parallel to that direction. This may lead to Moiré effects near the edges, with the same period as possible misfit-related strain fields.

Three other orientation relations for ZnO precipitates in Ag have been found. They only involve a simple rotation about the $[2\bar{1}\bar{1}0]$ axis of the ZnO precipitate, with respect to the Ag matrix. A common characteristic of the ORs is the parallel Ag [011] and ZnO $[2\bar{1}\bar{1}0]$ directions. Table 1 summarizes the characteristics of the orientation relations. Tilts increasing the angle between (0002) and (200) have been represented with a negative number. For all

Table 1. Angles between low index planes of Ag and ZnO facets of precipitates with OR1

	α'	α	β'	β
OR1	0	0	8.96	8.96
OR2	69.76	−0.78	62.34	8.19
OR3	−2.75	−2.75	6.21	6.21
OR4	−5.76	−5.76	3.2	3.2

α': angle between [0002] and [11$\bar{1}$]
α: angle between [0002] and closest ⟨111⟩ direction
β': angle between [01$\bar{1}$1] and [1$\bar{1}$1]
β: angle between [01$\bar{1}$1] and closest ⟨111⟩ direction

observed tilts this angle increases. The corresponding diffraction patterns are shown in Fig. 2.

The most prominent interfaces for OR1 are between the basal plane of ZnO and a close packed {111} plane of the metal. However, the edges of the precipitate are also faceted and the most important ZnO facets there are the first order prism and pyramidal plane. (The interfaces of the two sets of precipitates with basal planes parallel to the beam are equivalent, see Fig. 3.) These facets are also present on the OR2 and OR3 precipitates (Table 2), whereas the precipitate with OR4 showed no facets parallel to the viewing direction. Of course the orientation of the ZnO planes with respect to the matrix has also changed and, interestingly enough, neither OR2, OR3 nor OR4 causes any set of close packed planes to be parallel. In contrast, ORs for ZnO in Cu with ⟨2$\bar{1}\bar{1}$0⟩ and ⟨011⟩ parallel do show parallelism of close packed f.c.c. and ZnO planes. In that case {111}

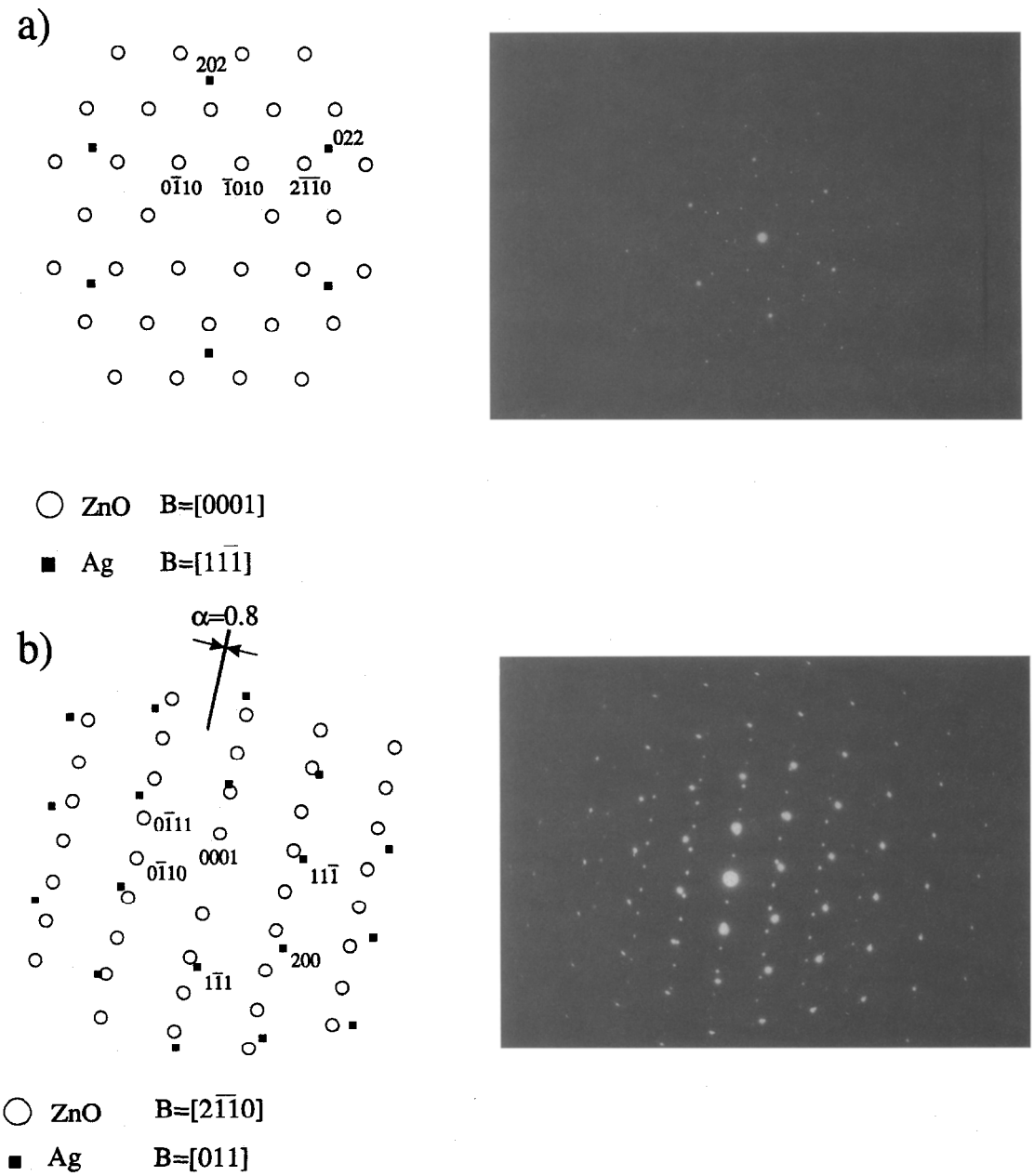

Fig. 2(a) and (b)

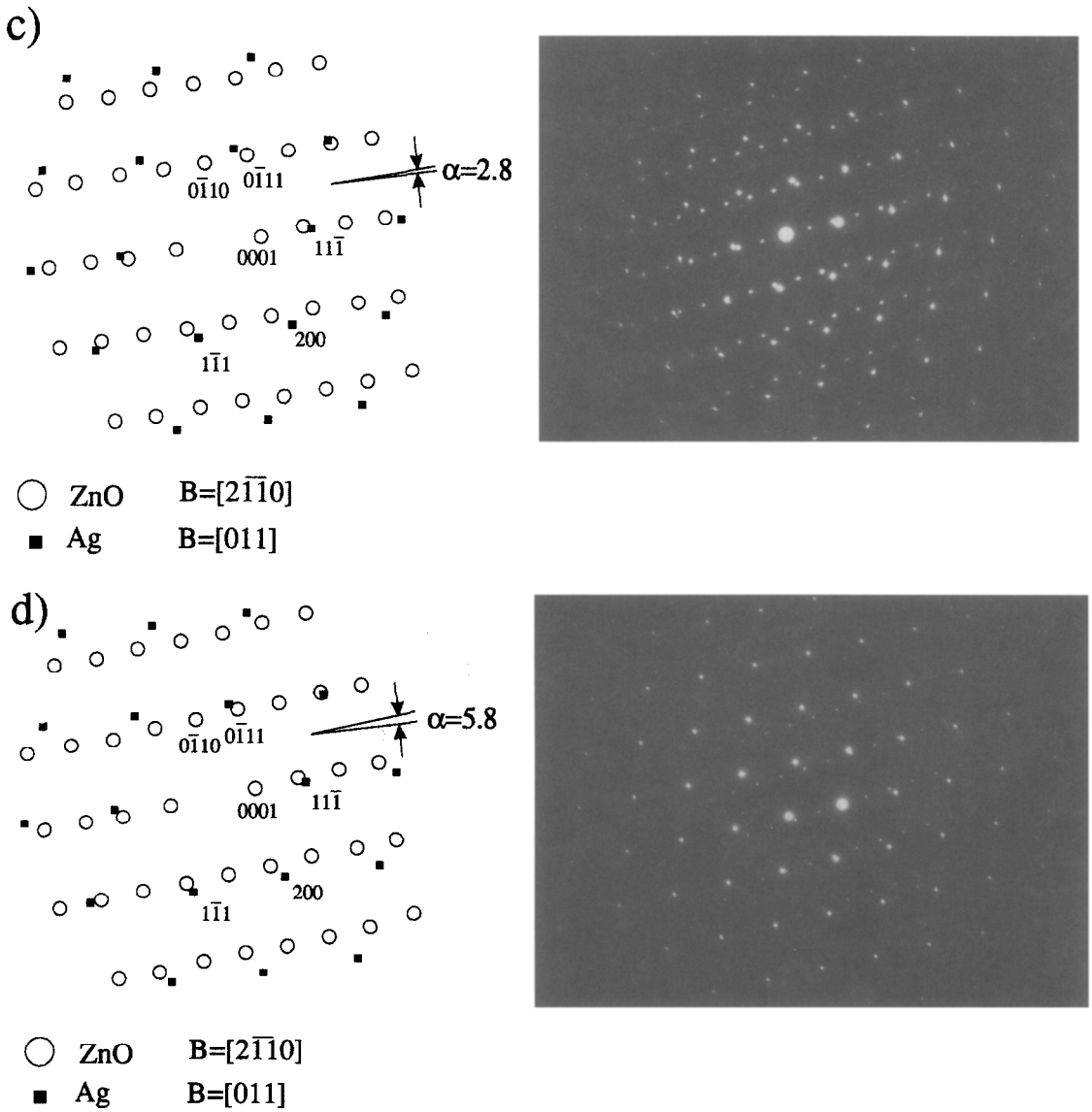

Fig. 2. Diffraction patterns corresponding to the orientation relations OR1 to OR4. (a) OR1; (b) OR2; (c) OR3; (d) OR4.

planes are either parallel with the basal plane or with a pyramidal plane. So, actually, the precipitates with OR2 and OR3 appear a little like the OR1 precipitates, sharing some of the important bounding planes. Comparison of the structure of these interfaces reveals the relaxations caused by the slight rotation in combination with the bonding on the interface structure.

4.2. HRTEM observations

As has already been mentioned, the edges of the wurtzite ZnO precipitates showed several types of facets. Among these interfaces only the $(01\bar{1}0)$ facet is parallel to a low index plane in Ag, the $(2\bar{1}1)$ plane. The pyramidal facets are not parallel to a low index plane in Ag. Furthermore, the difference in structure between the oxide and metal leads to the possibility that dissimilar interfaces involving the same ZnO facets exist. This should become apparent from Fig. 3 where the orientation of some important ZnO facets with respect to three sets of close packed metal planes is sketched. Clearly there is a possibility to find two different interfaces involving the first-order pyramidal ZnO interfaces. The abbreviation Py1 is used in the following, for the interface for which this smallest angle is between a pyramidal plane and a {111} plane. Py2 is used whenever the smallest angle is between a pyramidal plane and a {100} plane. The same distinction has been made for the tilted precipitates. The actual angles between the various planes differ of course, and have been tabulated in Table 3. There is a large difference between the structure of the interface at the Py1 and Py2 facets. The exact shape of the edges differs between any two precipitates. Facets are not always flat at an atomic scale, and do not have the same

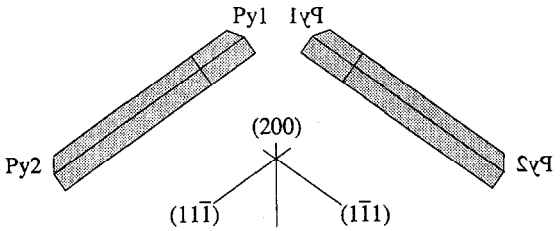

Fig. 3. Traces of low index f.c.c. planes, and examples of the two sets of precipitates with basal planes parallel to the beam, as viewed from [011]. Py1 and Py2 interfaces are indicated.

relative length on all precipitates. Some facets do not even occur on all precipitates.

On the basal plane the misfit of 1/2⟨110⟩ of Ag with the period of ZnO is about 12.4%. In fact there is an almost perfect match, within 0.1%, of 8 a_{ZnO} and 8 $a_{Ag}/\sqrt{2}$. The misfit is equal for all directions in the plane, as both surface nets are hexagonal. This also means that the misfit along the viewing direction for any interface considered here is 12.4%.

The geometry of the unrelaxed interface resembles those between f.c.c. metals and octahedral precipitates of oxides with NaCl-like structure, such as CdO and MgO. Model calculations, compared with results from HRTEM experiments on a Cu-MgO interface, were reported by us in a previous study [4]. We found that relaxations are likely to occur both along the interface and perpendicular to it, resulting in an interface structure with trigonal symmetry that may be interpreted as a network of (Shockley) partial misfit dislocations with edge character. The difference in stacking between the two cases is not expected to be of great importance for the interface structure so similar calculations on these interfaces are expected to give comparable results, see Fig. 4.

In the geometry forced upon it by OR1, the prismatic plane is parallel to (2$\bar{1}$1) in the metal. The misfit along this interface is large. If we take the repeat distances along the interface in both constituents we find a misfit of: (7.084/5.21) − 1 = 35%. Alternatively, we could take the misfit to be between distances of close packed planes along this direction; that is, disregarding the stacking sequence, and then we arrive at 10.3%. It is interesting to consider the nature of possible misfit dislocations at this interface relieving the misfit along the [11$\bar{1}$] direction. 1/2[01$\bar{1}$] lattice dislocations have a component parallel to the boundary of 1/3[11$\bar{1}$], and could relieve misfit. However, they also have a component perpendicular to the interface which would cause a tilt. An array of Frank partial dislocations near the interface would relieve misfit, without leading to a tilt.

Table 2. Low index ZnO facets parallel to [011] surrounding the precipitates

OR1	(002), (01$\bar{1}$1), (01$\bar{1}\bar{1}$), (01$\bar{1}$0), (01$\bar{1}$2)
OR2	(0002), (01$\bar{1}$1), (01$\bar{1}\bar{1}$)
OR3	(0002), (01$\bar{1}$1), (01$\bar{1}\bar{1}$), (01$\bar{1}$0)
OR4	no low index facets

Table 3. Smallest angles between close-packed planes of Ag and main facets of ZnO

		OR1	OR2	OR3	OR4
B	{111}	0	0.8	2.75	5.76
Pr	{111}	19.47	20.25	22.22	29.5
	{002}	35.26	34.48	32.51	25.23
Py1	{111}	8.96	8.18	6.21	3.2
Py2	{002}	6.84	6.06	4.09	1.08

Figure 5 shows a HRTEM image of a prismatic facet of a precipitate, in contact with the Ag (2$\bar{1}$1) plane. This boundary, although it seems to be straight in a global view, does not seem to show rigorously periodic features with the period one would expect. Bending of Ag (1$\bar{1}$1) planes in the region can be clearly seen though, and a step is indicated by the arrow. As is evident from HRTEM images, presented in Figs 6 and 7, both pyramidal interfaces Py1 and Py2 sketched in Fig. 3 can be found. Figure 8 depicts a rigid lattice model for both boundaries. The fact that both appear does not necessarily indicate that the energy difference between the two structures is small. A precipitate might still show more of one interface than of the other. In fact the trigonal rather than the hexagonal shape of the precipitates may point in that direction. In Fig. 1, it is indicated what the precipitate might look like. Here, an energy difference is assumed to cause unequal areas of the interfaces to appear. This hypothesis could of course be verified by imaging both sides of a precipitate at once. However, the precipitate shape in Fig. 1 is an idealized one; in reality the precipitates are not all exactly alike, and the situation is therefore not as clear-cut. Py1 shows the pyramidal facet of ZnO making an angle of 8.9° with the (1$\bar{1}$1) Ag plane. As the geometry of the interface is really determined by the parallelism of (11$\bar{1}$) and the basal plane, we do not have to look for deeper reasons behind the angle of 8.9°. What is interesting, however, is to see how the structure of the silver and ZnO has adapted to this peculiar situation. Looking at the hard sphere representation, we might interpret the structure as a stepped silver surface in contact with a ZnO pyramidal plane. The steps in the Ag are 1/4 ⟨211⟩ type steps. The projections of these steps perpendicular to and along the interface are 1/3 ⟨111⟩ and 1/12 ⟨211⟩, respectively. From the experimental image it is clear that at the actual interface these steps are no longer distinguishable as such and appreciable relaxations have occurred. The relaxation evidently involves the creation of a partial dislocation on the (1$\bar{1}$1) plane, which has moved somewhat from the interface leading a small area of the stacking fault. Py2 is 6.835° off parallelism of the pyramidal plane with the Ag (200) plane. This interface can also be constructed using 1/4 ⟨211⟩ steps, but in this case the projections perpendicular to and along the interface measure 1/2 [100] and 1/4 ⟨011⟩

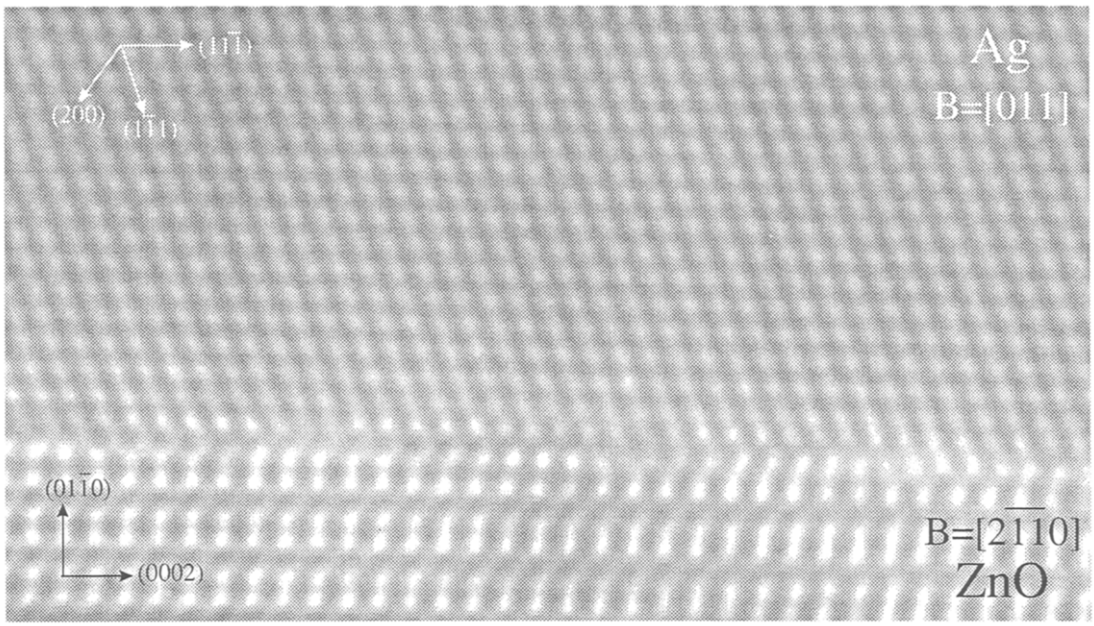

Fig. 4. HRTEM image of basal plane of ZnO in contact with Ag (11$\bar{1}$). Defocus is about −48 nm.

respectively. As in the former case, small areas of the stacking fault seem to be present near the interface, judging from the experimental micrographs. Now there are two available {111} glide planes present, with a 6.8° difference in angles between them and the interface. It can be seen that the {111} plane making the largest angle with the interface is the glide plane involved. In the course of our investigations focus has been on interfaces coinciding with low index ZnO planes, but we also encountered some situations where an interface on the edge involved a clearly and periodically stepped ZnO plane.

For the precipitate with OR2 a {01$\bar{1}$1} plane is found on the precipitate, and also a very short {0002} segment. Another pyramidal facet was present, but a groove formed along it during ion milling, effectively creating a hole. All other interfaces appear not to be parallel to the beam, or curved. HRTEM images of some of the interfaces surrounding this precipitate are shown in Figs 9 and 10. Figure 9 shows the interface

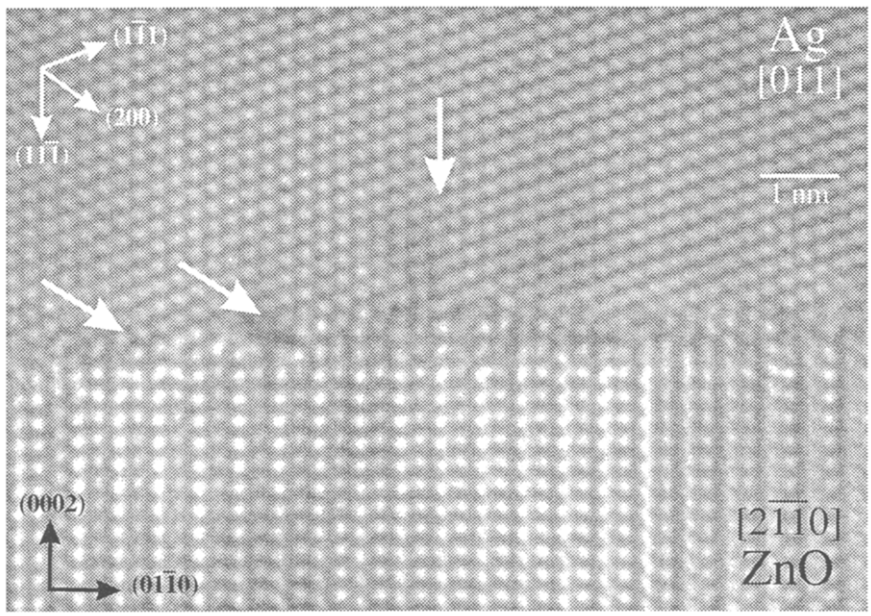

Fig. 5. HRTEM image of a prismatic facet of ZnO in contact with Ag. Steps are indicated on the left-hand side of the image. A dislocation core is indicated by the arrow pointing downward. Defocus is about −48 nm.

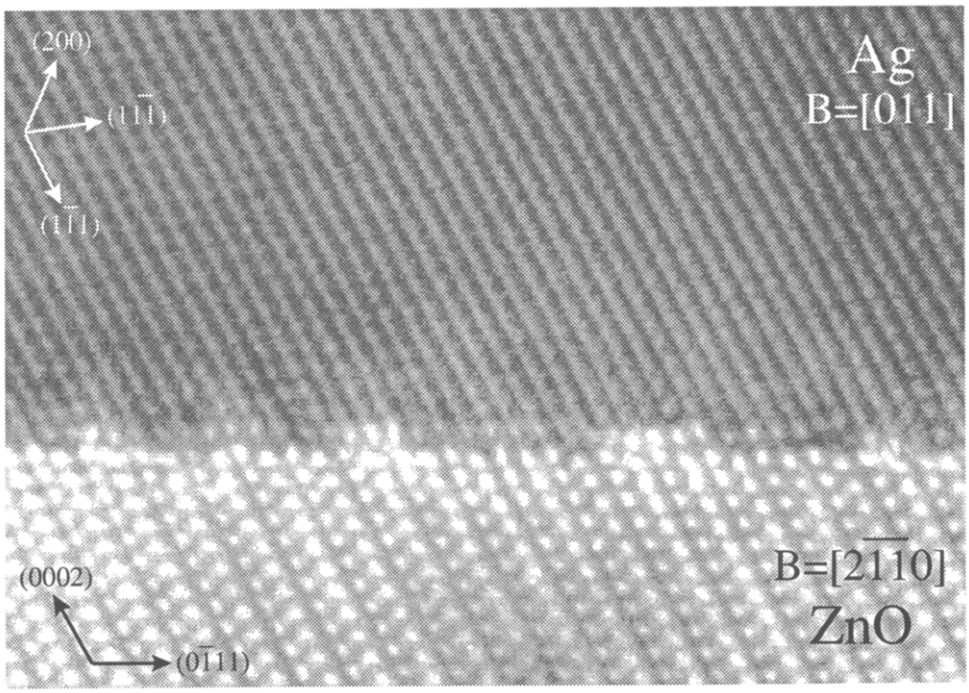

Fig. 6. HRTEM image of a Py1 interface. The first-order pyramidal plane of ZnO makes an angle of 8.96° with the Ag (1$\bar{1}$1) plane. The image suffers from a rather large tilt present during exposure. Only one set of fringes is clearly visible in the Ag. Nevertheless, the appearance of the other set of fringes is clearly different near the interface, as compared with the bulk pointing to relaxations. Defocus is about −48 nm.

with the basal plane of ZnO. The angle between the basal plane and the (11$\bar{1}$) plane is about 0.8 ± 0.5°. If there is no homogeneous strain on this interface a 1/4⟨211⟩ step is needed every 17.3 ± 10 nm to arrive at this angle. The measured distance between the faulted parts in the figure is about 9 nm. This facet was rather short and this was the only part that yielded clear images. The two faulted parts, clearly visible in the figure, are far more evident than at the basal plane interface of OR3. It is unclear whether the stacking faults visible have originated at the interface or have slipped to the interface. From the image it is clear that the (11$\bar{1}$) planes between the stacking faults are parallel to the interface, whereas they are tilted with respect to it only at a larger distance. The interface between the stacking faults, therefore resembles the interface of the basal plane of the precipitate with OR1. In this case, there are "domains" at the interface, separated by the stacking faults. The Ag lattice points in consecutive "domains" are translated by $1/6\{121\} \times a_{Ag}$, which means that the misfit dislocation network has also been translated, by $1/6\{121\} \times a_0$, where a_0 is the period of the network. For the misfit dislocation network, the lines of intersection of the stacking faults with the interface therefore also act as "domain boundaries".

Figure 10 shows the Py1 interface. The angle between the pyramidal plane and the (1$\bar{1}$1) plane is about 8.2 ± 0.5°. If there is no homogeneous strain on this interface a 1/4⟨211⟩ step is needed every 1.65 ± 0.1 nm to arrive at this angle. The measured distance is 1.9 ± 0.2 nm and is in agreement with the expected value.

In the case of OR3, three surfaces of the ZnO precipitate are the same as for OR1, and in fact this precipitate looks a lot like an OR1 precipitate slightly rotated in the matrix. The shared planes are {0002} and {01$\bar{1}$1}, and {01$\bar{1}$0}. The orientation of this precipitate in the matrix is different from that of the OR2 precipitate. Its (0002) is almost parallel to (1$\bar{1}$1) instead of (11$\bar{1}$). Moreover, the sense of rotation is inverted, but this means that it increases the angle between (0002) and (200), just as for OR2. As a consequence, the interfaces can be modelled with the same steps as the interfaces for OR2. With the other sense of rotation, the interfaces involving planes close to a {111} plane would have shown steps with 1/2⟨110⟩ character instead of 1/4⟨211⟩.

Figure 11 shows the interface with the basal plane of ZnO. The angle between the basal plane and the (11$\bar{1}$) plane is about 2.7 ± 0.5°. The component of the 1/4⟨211⟩ step perpendicular to the interface is 1/3⟨111⟩ in this case. This component gives rise to the tilt. If there is no homogeneous strain on this interface a 1/4⟨211⟩ step is needed every 4.92 ± 0.9 nm to arrive at this angle. A lower density of steps would mean that long range stresses are present, either coherency stresses or residual stresses. The measured distance is about 5.2 ± 0.5 nm, which is in agreement with the expected value. However, as already indicated by the rather large error, the

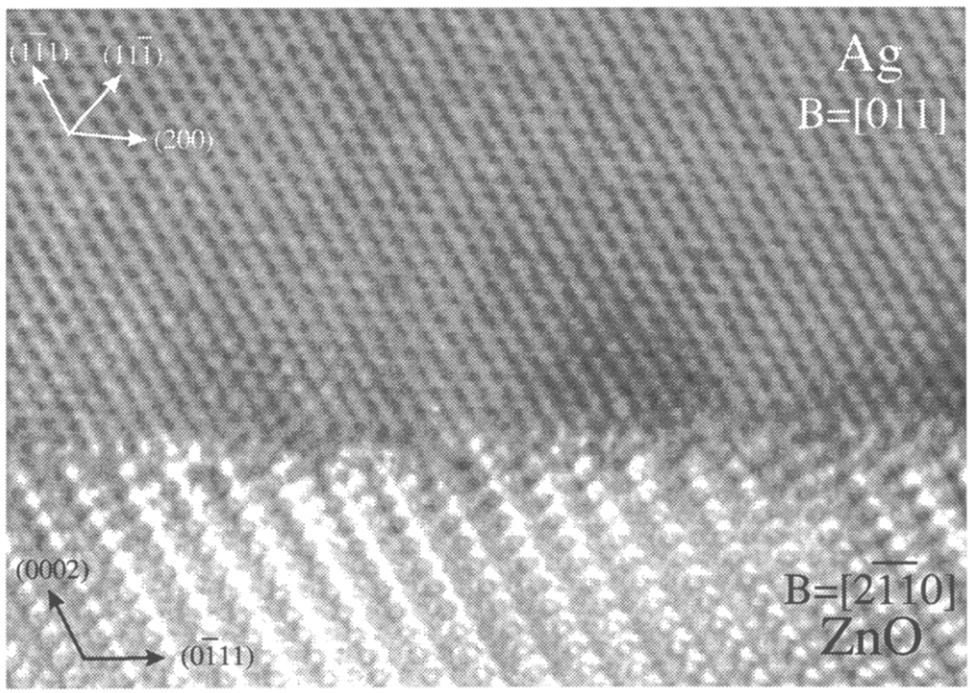

Fig. 7. HRTEM image of a Py2 type interface. The pyramidal plane of ZnO makes an angle of 6.84° with the Ag (002) plane. The image of the interface is not very clear. Bending of the planes near the interface may, however, point to relaxations. Defocus is about −48 nm.

periodicity of the steps at the interface is not perfect. A certain irregularity is expected because the distance between the steps is not an integer multiple of the periodicity of the Ag along the (untilted) interface. This effect may cause a step to appear after 20 or 19 instead of 19.64 1/4⟨211⟩ distances, but is not expected to lead to the large difference we see here. At this interface, distortions in the ZnO seem to accompany the relaxations in the metal. For the structure of the misfit dislocation network that may be present at this interface the same remarks apply as for the basal plane interface of OR2. Figure 12(a) shows the Py1 interface. For the Py2 interfaces the component of the 1/4⟨211⟩ step giving rise to the tilt is 1/3⟨111⟩. The angle between the pyramidal plane and the (1$\bar{1}$1) plane is about 6.2 ± 0.5°. If there is no homogeneous strain on this interface a 1/4⟨211⟩ step is needed every 2.24 ± 0.2 nm to arrive at this angle. The measured distance is about 2.1 ± 0.1 nm, so no homogeneous strain is thought to be present at the interface. Figure 12(b) shows the Py2 interface. The angle between the pyramidal plane and the (200) plane is about 4.09 ± 0.5°. Relaxations near the interface are clear when it is viewed along the (200) planes. The picture does not show a clear periodicity along the interface. Figure 13 shows the prismatic interface. Displacements are evident looking along, for example, the (1$\bar{1}$1) planes. Compared with the prismatic plane interface of precipitates with OR1, Fig. 5, it shows less steps. The interface is atomically flat over about 50 nm. Relaxations are evident near this interface as a view along, for example, the (1$\bar{1}$1) planes will show. Three cores of interface dislocations are indicated by arrows in the figure.

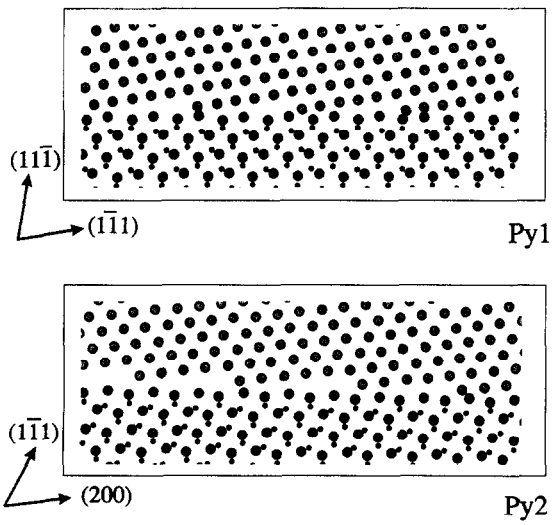

Fig. 8. Hard sphere representation of the Py1 and Py2 interfaces. Note the different projections of the steps in the metal parallel and perpendicular to the interface.

In conclusion, we have observed interfaces between low index ZnO facets, and several high index Ag planes. On the interfaces with high index Ag planes, interfaces with "tilt", relaxations were observed in all cases. The tilt can be modelled with an array of 1/4⟨211⟩ steps on the metal side of the

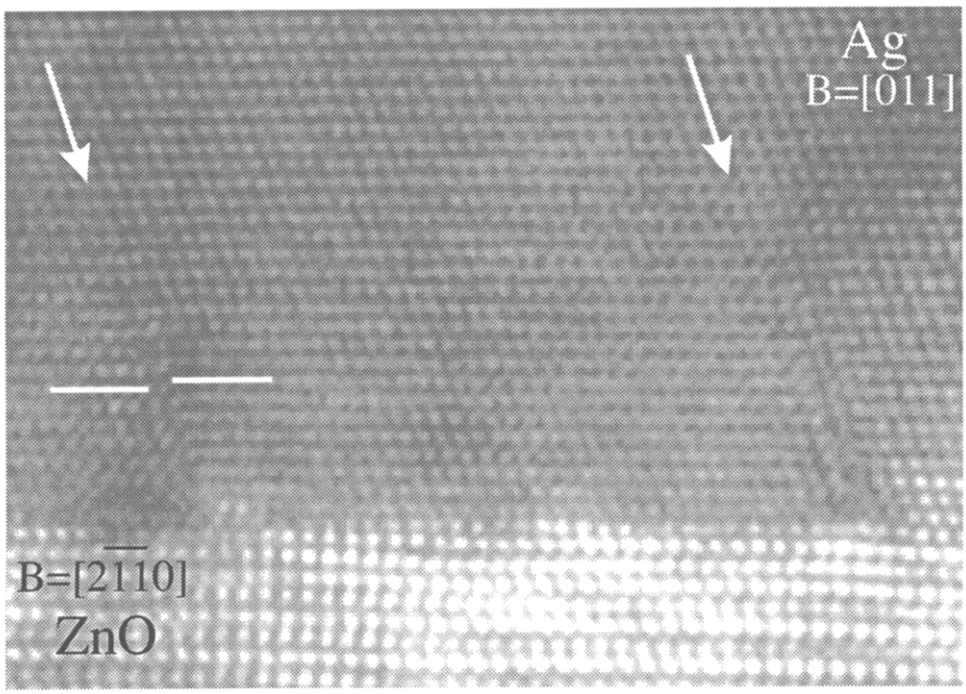

Fig. 9. HRTEM image of the basal plane interface of a precipitate with OR2. Two stacking faults on the (11$\bar{1}$) plane are indicated by arrows. Note that the (1$\bar{1}$1) planes between the stacking faults are parallel to the interface, whereas above them they are under a slight angle of about 1°. Defocus is about −24 nm.

interface, either on a {111} plane or on a {002} plane. Relaxation of these steps was most prominent on interfaces involving a {111} plane slightly tilted with respect to the interface. A common characteristic of these relaxations is the appearance of a stacking fault on the {111} plane intersecting the interface with the largest angle.

Apart from the precipitates of hexagonal ZnO, the internally oxidized Ag-Zn alloys also contain precipitates of ZnO with the sphalerite structure.

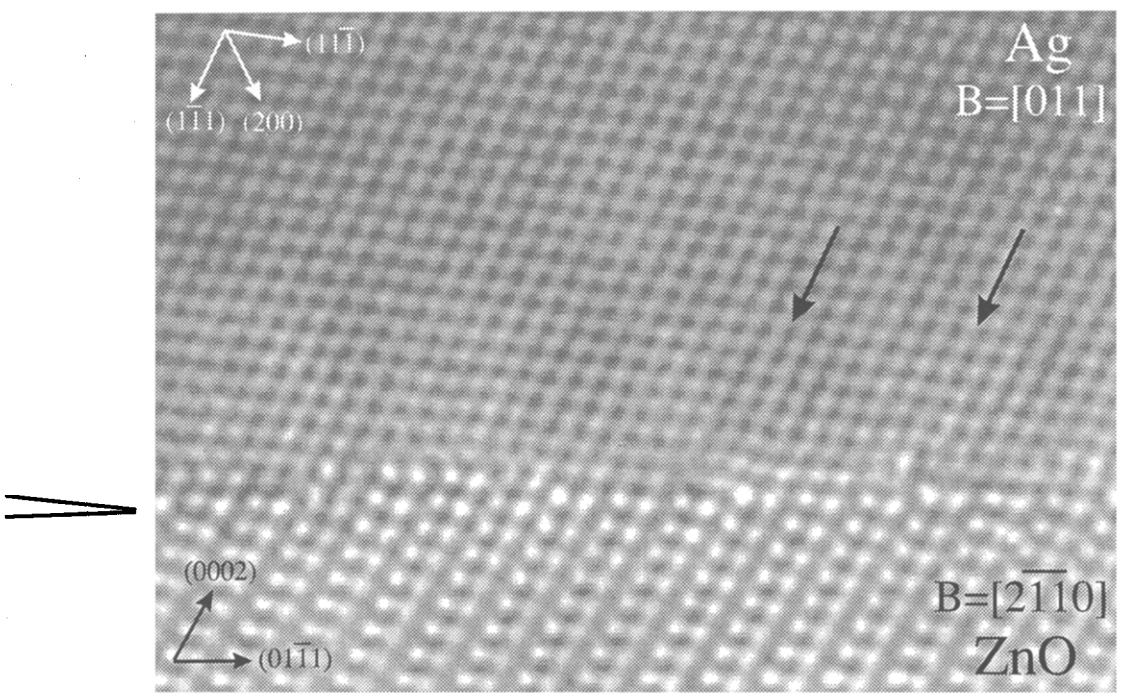

Fig. 10. HRTEM image of a Py1 interface of a precipitate with OR2, relaxations are clearly visible looking along the interface. Arrows point to cores of the dislocation structure. Defocus is about −24 nm.

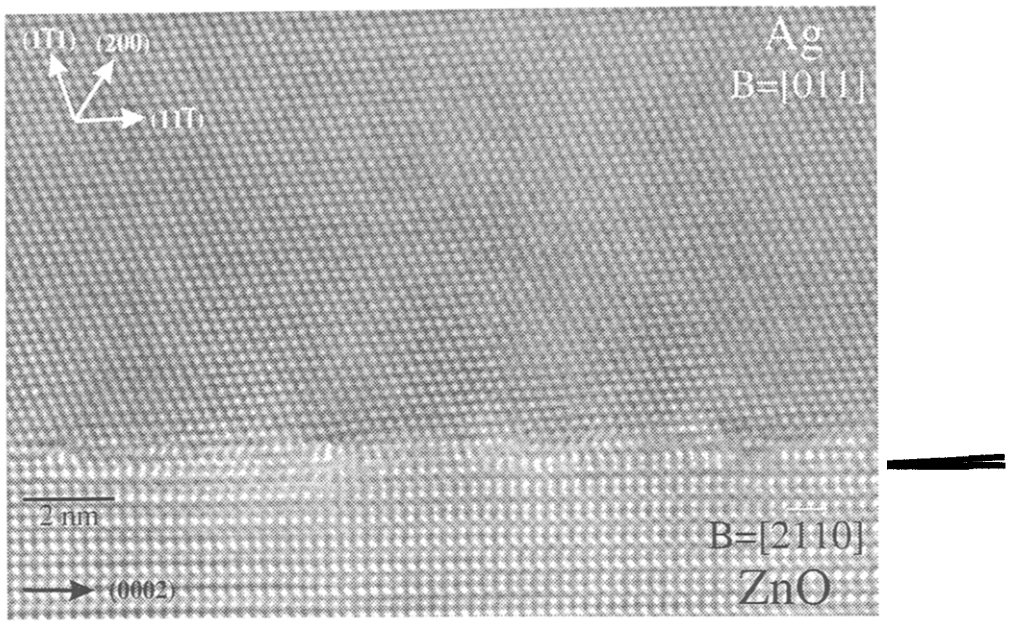

Fig. 11. HRTEM image of the basal plane interface of a precipitate with OR3. Looking along the interface an array of dislocations can be seen. Defocus is about −12 nm.

Evidence for the existence of this phase in our samples is presented in Fig. 14. Diffraction patterns of three zones taken from the same precipitate, or rather group of precipitates, are shown in Figs 14(b), 14(c) and 14(d). The diffraction patterns from the $\bar{1}21$ and the $\bar{1}11$ zone axes are selected area diffraction patterns, showing only spots of Ag and the cubic phase. The diffraction pattern from the 011 zone also shows spots from the two hexagonal precipitates viewed along $2\bar{1}\bar{1}0$ zone axes.

All spots that cannot be attributed to Ag or hexagonal ZnO, can be accounted for if a cubic form of ZnO is assumed to be present.

The bright field images in Figs 14(a) and 14(e), give a more appealing view of this phase, and strongly suggest the sphalerite character. These precipitates were always found in close contact with two or more precipitates of hexagonal ZnO, meeting on close packed planes: {111} in the case of the cubic phase, {0002} in the case of the hexagonal phase. The precipitates show stacking faults, and there are even slabs with a hexagonal structure inside them. This disorder in the stacking of {111} planes leads to a star-shaped diffraction point, with arms in the direction perpendicular to the {111} planes. This leads to streaking in the 011 zone axis DP and the appearance of satellite spots in the $\bar{1}11$ and $\bar{1}21$ zone axis DP.

5. DISCUSSION

5.1. *Sphalerite ZnO*

The presence of the metastable ZnO phase in the internally oxidized alloy needs a physical explanation. Metastable phases have been encountered on several other occasions after internal oxidation. They involve (mostly) cubic aluminium oxides in copper [21, 22] or niobium [23], and also oxides of manganese in copper [24] and silver [9], although the latter case must be doubted [25]. Of course, this phenomenon has a close analogy in other processes involving nucleation and growth within solids. The transition phases may occur because the nucleation barrier for them is lower than for a direct formation of the stable phase. The lowering of the nucleation barrier is a consequence of the lower interfacial energy of the transition phases compared with the stable phase. After nucleation, the metastable phase may grow until the Gibbs free energy gets higher than that of a precipitate with the stable phase. In general, the change in free energy ΔG when a new phase of volume V_β and an interface A_β forms, causing an increase in elastic strain energy per unit volume $\Delta G_{\text{el}}^{\text{V}}$ is given by:

$$\Delta G = V_\beta \Delta G_{\alpha\beta}^{\text{V}} + A_\beta \gamma_{\alpha\beta} + V_\beta \Delta G_{\text{el}}^{\text{V}},$$

where $\Delta G_{\alpha\beta}^{\text{V}}$ is the free energy per unit volume. We would expect nucleation of sphalerite instead of wurtzite if the following condition is met:

$$(V_{\text{Sph}} \Delta G_{\text{Ag-Sph}}^{\text{V}} - V_{\text{Wu}} \Delta G_{\text{Ag-Wu}}^{\text{V}}) \leq A_{\text{Wu}} \gamma_{\text{Ag-Wu}} - A_{\text{Sph}} + V_{\text{Wu}} \Delta G_{\text{el-Wu}}^{\text{V}} - V_{\text{Sph}} \Delta G_{\text{el-SSph}}^{\text{V}}$$

If the energy of formation of sphalerite inside the Ag matrix is more positive than of wurtzite, i.e. in accordance with the Gibbs free energy of formation, the term on the left is positive, expressing the deficit in energy of a volume of sphalerite with respect to an equal volume of wurtzite (1.9398×10^{-3} eV/Å^3 [16]). A lower total interface energy and strain energy term

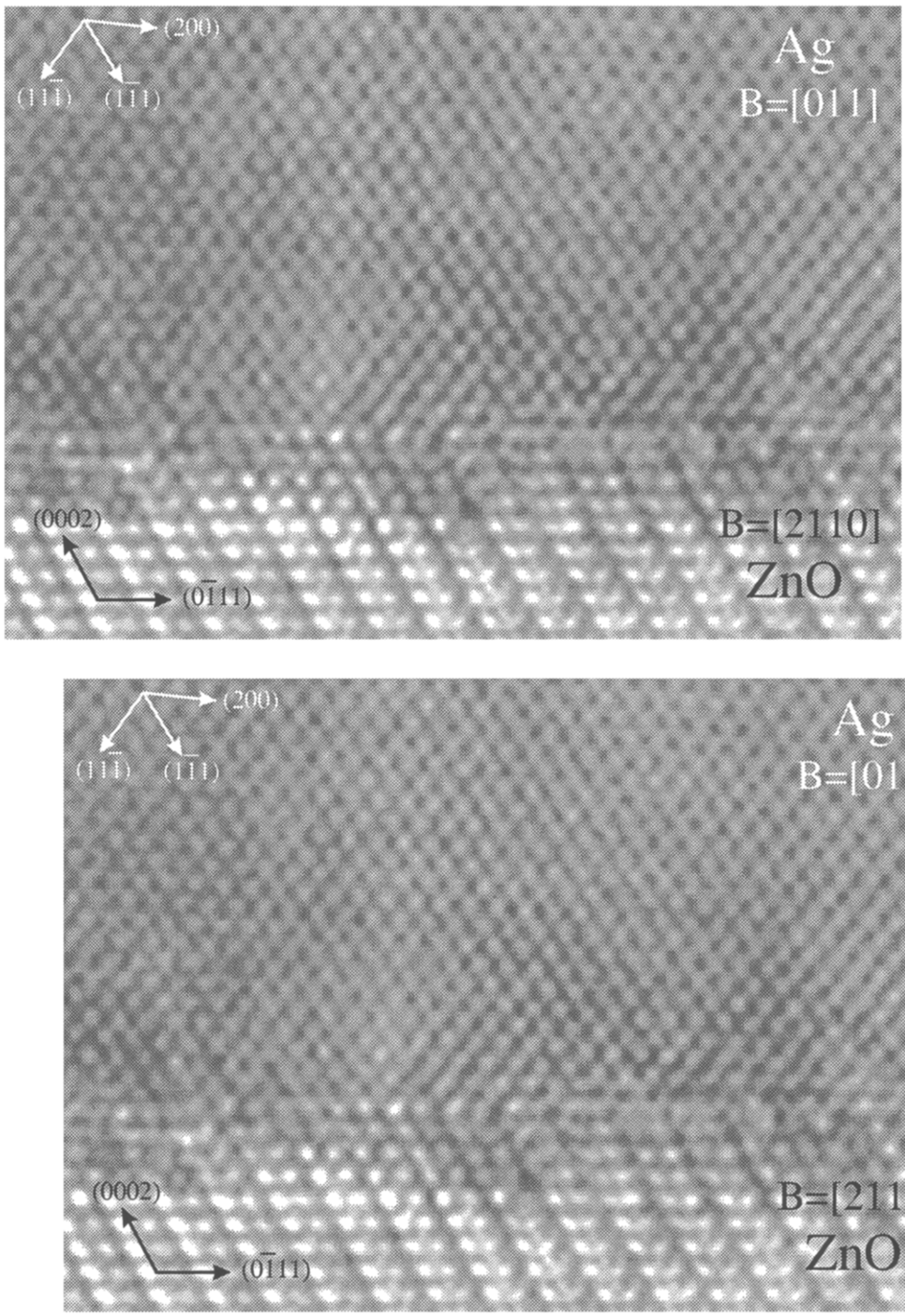

Fig. 12. (a) HRTEM image of an interface involving a Py1 pyramidal plane of a precipitate with OR3. Defocus is about −36 nm. (b) HRTEM image of an interface involving a Py2 pyramidal plane of a precipitate with OR3. Near the interface, relaxation of the (002) planes can be seen. Defocus is about −36 nm.

for the sphalerite are thus needed to make nucleation possible. A first thought, regarding the interface energy term, leans somewhat on negative evidence, namely that until now we have not found any cubic ZnO precipitates in Cu. We could assume therefore that a nucleus of cubic ZnO is less stable in Cu than in Ag. We have already noted that there exists a slight difference in ionicity between the two compounds, and that the resistance of Cu is larger than that of Ag. Screening of the ionic compound will be somewhat more efficient in Ag, effectively reducing this particular difference between small nuclei of the

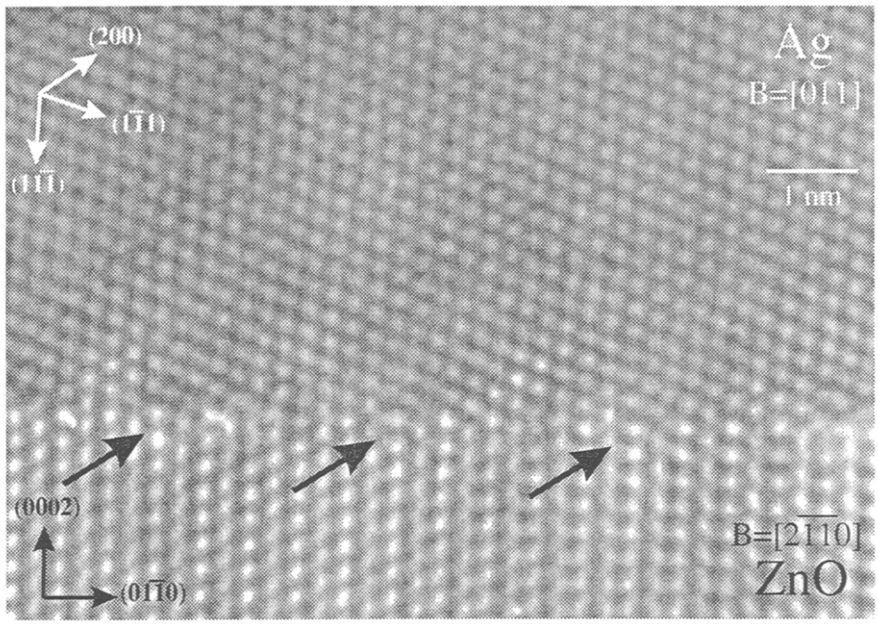

Fig. 13. HRTEM image of an interface involving a pyramidal plane of a precipitate with OR3. Defocus is about −24 nm.

two phases. One might argue on these grounds that it is more likely to find both wurtzite and sphalerite in Ag, than in Cu. Further it has to be emphasized that the interface energy term is quite important for the nucleation rate as well. In the case of homogeneous nucleation it is easy to see that the rate of nucleation is proportional to the power cube, i.e. proportional to $\exp[-A\gamma^3]$, where A depends on $\Delta G^{\mathrm{v}}_{\alpha\beta}$ and $\Delta G^{\mathrm{v}}_{\mathrm{el}}$. However, the question should be addressed whether we are dealing with homogeneous precipitation in the first place.

The cubic form may be in contact with the silver, and does not have to be completely surrounded by hexagonal precipitates. (In fact, we also observed an interface between {111} planes of ZnO and Ag.) Starting with the nucleation we observe that two wurtzite plates that grow on different {111} planes may meet. The angle between them can be either sharp or obtuse. If the angle is sharp, the line of intersection seems to be a likely spot for the sphalerite to nucleate heterogeneously, as the interface energies with the two wurtzite precipitates are expected to be very low. Furthermore, if the wurtzite precipitates were to grow further inward a high energy grain boundary would form, much like the one visible in Fig. 14. The slight deviation of the ideal c/a ratio for hexagonal ZnO means that the possible symmetric boundary would not be exactly parallel to the $\{01\bar{1}0\}$ planes in the ZnO, which could have provided a good fit and a relatively low energy grain boundary. Instead, this grain boundary is expected to have a relatively high energy. If the two precipitates grow, this same misfit will ensure that at a certain instant of time the local situation will be exactly that of the cubic structure, which then might start to grow. We could consider the surrounding of the sphalerite by wurtzite as a kind of three-dimensional epitaxy. In most cases found, three and perhaps even four low energy interfaces surround the sphalerite form. The cubic sphalerite structure fits perfectly in the space between the hexagonal precipitates, so no deformation strains have to be present in the inclusion. In this picture the cubic Ag matrix plays an important role, providing the correct angles.

Because we have always found the sphalerite and wurtzite structure together, this suggests that only sphalerite precipitates that nucleate heterogeneously in this particular way can be stable, and even that this is the only way the sphalerite may form. It should be borne in mind that the appearances of the interfaces are considered here more or less exclusively from the energetic point of view, disregarding the effects of kinetics. As a matter of course, in internal oxidation, kinetics also play an important role. Precipitates may grow faster parallel to an interface that has a relatively high energy. Similarly, ledges along the interface may promote particle growth and the growth process may be determined by diffusion across kinks in the ledges [26]. The main oxidizing conditions influencing the nucleation and growth of the precipitates are the temperature of the sample, the oxygen partial pressure, the concentration of the solute and the oxidizing time. Systematic investigations of the effect of these parameters on the microstructure of the internally oxidized alloys are possible using an adapted Rhines pack method in which sample temperature and oxygen pressure are independently controlled [27]. It seems that no systematic studies have been carried out so far on the effects of the oxidation parameters on the morphology and on the

a)

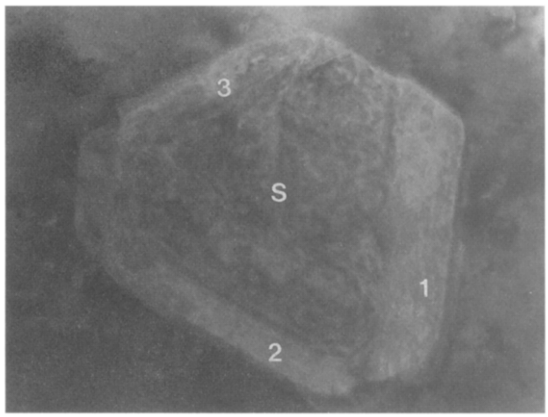

100 nm

b)

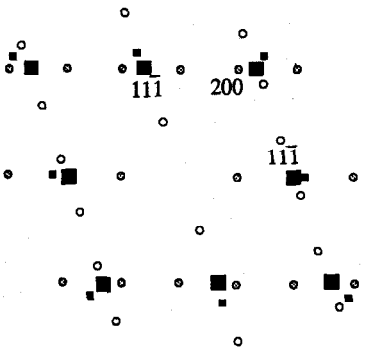

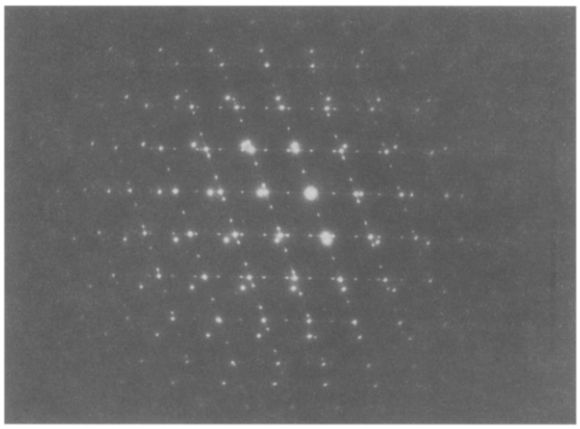

ZnO_{cub} B=[011]
$ZnO_{hex\ 1,2}$ B=[$2\bar{1}\bar{1}0$]
Ag B=[011]

c)

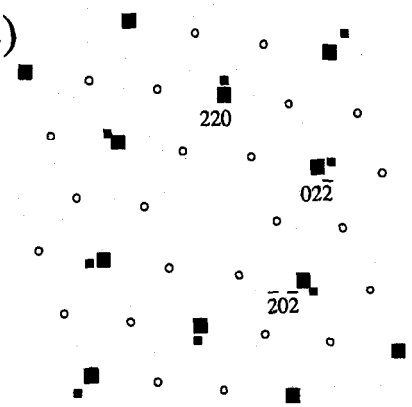

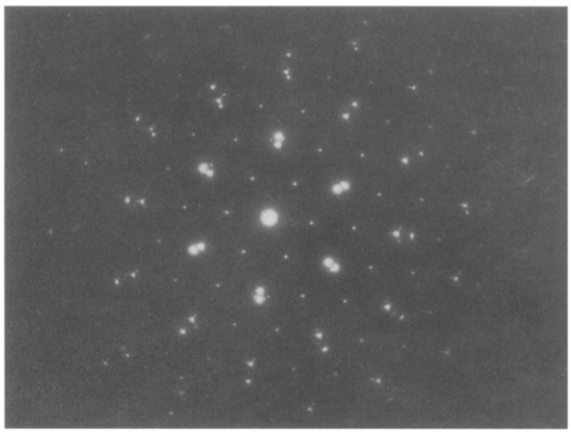

ZnO_{cub} B=[$\bar{1}$11]
$ZnO_{hex\ 3}$ B=[0001]
Ag B=[$\bar{1}$11]

Fig. 14(a)–(c)

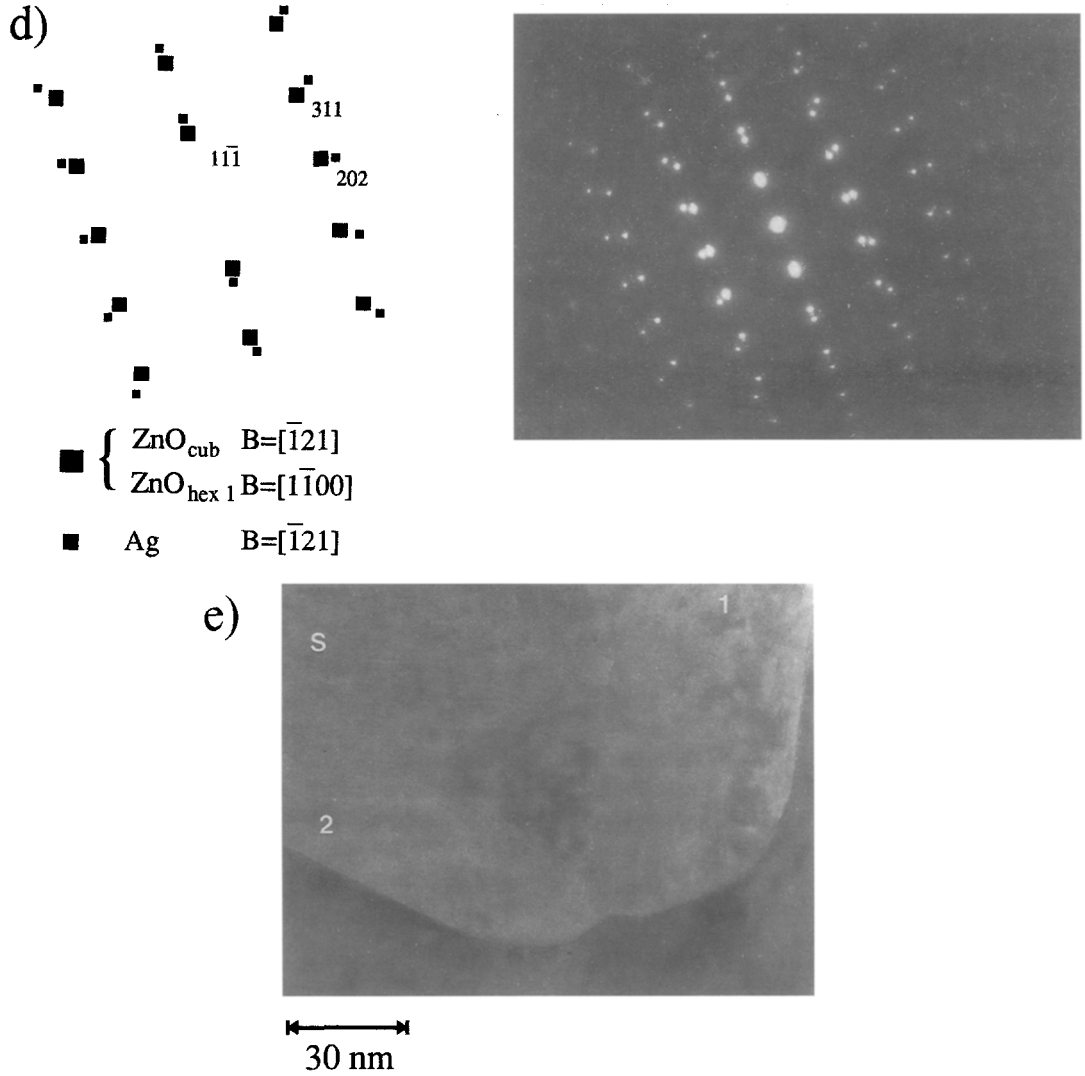

Fig. 14. (a) A sphalerite ZnO precipitate, surrounded by three wurtzite ZnO precipitates, labelled 1,2,3. The HRTEM image in (e) is from the [011] zone of the sphalerite ZnO grain. Diffraction patterns from three zones are shown in (b), (c) and (d).

size of the oxide precipitates, and not on the formation of ZnO precipitates, using HRTEM. These aspects are considered in a subsequent paper [10].

5.2. "Tilted" precipitates

Precipitates and interfaces with small misorientations from a preferred OR are an interesting phenomenon. Similar cases have been reported in the literature for widely differing interfaces produced with various methods. In addition, their presence is not restricted to metal–oxide interfaces. A short review of the most important findings follows and their relationship to the case at hand is discussed. The reason for the existence of a tilt, similar to that described here, has been explained convincingly in two cases. First, in a series of experiments on strained epitaxial layers, Flynn and coworkers showed that the tilt of the layer is such that it leads to a complete strain relief of the epitaxial layer. They used purely geometrical arguments, and an assumption about the coherency strains at the interface to arrive at this conclusion [28–30]. As a consequence of the tilt the low energy coherent interface is replaced with a higher energy interface. If this were not the case the tilt should have been present all along. In two other cases strain relief seems not to play a role in the existence of a tilted interface. Thin layers of Nb and V grown on the R plane of sapphire show a tilt of a few degrees. However, in these systems a unique three-dimensional orientation relation is found for growth of many sapphire surfaces, which also applies to these particular cases. The tilt is here attributed to favourable interactions between the substrate metal ions and the metal atoms in the epitaxial layer. The lattice of the epitaxial layer can be thought of as a continuation of the metal sublattice in the sapphire. The energy of these particular tilted interfaces is taken to represent a (local) minimum [31, 32].

These cases have in common that the tilt angles found were unique for each system. This is reflected in the explanation of their occurrence, which does not allow for other tilts to be present. This is clearly different from the situation we encountered. Apart from a, quite large, number of seemingly isolated cases [33–37], there are a few recent observations that compare well to our case in that they show a number of tilt angles for the same system.

Internal reduction of $(Al,Cr)_2O_3$ leads to the formation of Cr precipitates in a sapphire matrix [5]. Roughly, there are two sets of ORs. One OR is actually a narrow range of ORs related to each other by a simple rotation of up to about 5.5°. The two limiting cases correspond to situations showing parallel close packed planes, and these cases are encountered most frequently. Distribution between them is more or less continuous, perhaps showing another small peak. No explanation is given for the occurrence of the tilted precipitates.

In another study, an orientation relation for Al_2O_3 precipitates in Pd was found to occur with misorientations from the exact relation of up to 11°. In this range, precipitates with four different morphologies were found. For all these precipitates the angles between sapphire facets and close packed Pd planes were below 7° [38, 39]. A distribution of tilt angles, based on measurements of roughly 75 precipitates shows a broad peak around a certain angle, which is taken to mean that facets of particularly low energy are present at that angle. Two of these facets show parallelism of rather low-index sapphire and Pd planes, and one is "tilted" and shows a good fit of one period in the tilted Pd and four periods in the sapphire. In this case, HRTEM images did not show clear evidence of relaxations near the interface. The exact value of the tilt angle is explained in a way analogous to the strain-relief of the epitaxial layers mentioned before. It is interesting to compare our findings with the results of Cosandey *et al.* [39]. In our case, almost all precipitates show OR1, and this can safely be considered to be the low energy configuration. The ORs we found do not show parallel low index planes at all, which is remarkable. Considering these precipitates to have a preferred orientation would obviously require an explanation of some sort. We cannot conclude from our measurements that there is a preferred "tilted" orientation because we simply lack data, mainly because the tilted precipitates are very rare. We might look for such an angle without unambiguous experimental backing as Cosandey *et al.* have found, but prefer not to. It would, it seems, have a lot in common with applying two criteria that have been put forward in the past to predict low energy interfaces: high planar density of (near) coincidence sites [40], or high density of "locked-in" rows at the interface [41]. These criteria, appealing as they may seem in this case, have been shown to be not reliable in determining which interfaces have low energy [42]. Especially in cases where substantial relaxations take place, geometrical models basically cannot be expected to predict variations in interface energy. The situation is even more complicated because several interfaces are involved at the same time here.

Looking for a more general explanation of the occurrence of these precipitates we note the following. In the tilted precipitates, the perfect alignment of the basal plane with a {111} plane is destroyed. This is the most frequently occurring interface, not only in this system but also for ZnO in Cu and Pd, that is to say, in cases with a different bonding and a different misfit. Therefore, it probably has a particularly low interface energy. Tilt will thus lead to an increase of the interface energy of this facet. Furthermore, it destroys the symmetry at the interface. This, together, makes it very unlikely that this facet causes the tilt. The situation is different for the other facets found on OR1. For all these facets the tilt axis is along a unique direction in the interface. If, during precipitation coherency, strains occur at these interfaces they will be strongly anisotropic, in contrast to possible strains at the basal plane. These coherency strains may be relieved by the glide of lattice dislocations to the interface, causing the tilt, or by the nucleation of dislocations at the interface as discussed in [43]. So, relief of coherency strains at these interfaces may have played a role in the formation of these precipitates. In OR1, these interfaces are not expected to have very low energy, because the angle the Ag planes make with them are fixed by OR1. An interface with Ag planes at slightly different angles may have a lower energy, increasing the driving force for tilt. Finally, we note that the angles between the two pyramidal facets and low index planes are both decreased by the tilt, as becomes clear from Table 3. As the measurements of Cosandey *et al.* [39] indicate that "low-angle" interfaces are preferred over "high angle" interfaces, this may be of importance.

Next, we turn to the structure of the tilted interfaces. The tilted interfaces between Ag and ZnO, including the Py1 and Py2 interface of OR1, all seem to show relaxations near the interface. An unrelaxed tilted interface is characterized by an array of steps on the metal side, causing the macroscopic angle. At the pyramidal interfaces these are $1/4\langle 121\rangle$ steps in the Ag. These may be interpreted as the projection of a $1/2\langle 110\rangle$ vector. A perfect lattice dislocation sliding along a {111} plane towards an interface, would, upon reaching it, leave such a step. The dislocation line is inclined to the interface during the sliding. This observation holds for the steps on both the Py2 and Py1 interfaces. The only difference is the projection along and perpendicular to the interface. Another interpretation is to regard the steps as introduced close packed planes. For the Py1 planes we can interpret the steps as introduced {111} planes. In this way, the interface resembles an array of $1/3(11\bar{1})$ Frank partial dislocations, with line direction [011].

A similar interpretation of the Py2 interface would lead to an image involving inserted (200) planes or partial 1/2[100] edge dislocations with the line direction along [011]. No equivalent in the f.c.c. structure is known, as it would create a stacking fault with very high energy. The Burgers vector attributed here to the steps is derived from the metal, not from the ZnO. This is only justified if the ceramic is taken to be rigid. In that case, the complete Burgers vector will still be at the metal side. Under these circumstances, we can use the picture to illuminate the effects of relaxation on the distribution of the Burgers vector near the interface. The experimental data suggest that a dissociation of the Burgers vector, or steps, takes place. More specifically, the "terraces" tend to align with the interface, creating a small stacking fault at the place of the steps. We interpret this as a dissociation of the Frank partial dislocations at the interface into $1/6[21\bar{1}]$ Shockley partial dislocations and a $1/6[01\bar{1}]$ stair-rod dislocation. The Shockley partial dislocations can glide up the available $(1\bar{1}1)$ plane, away from the interface whereas the "stair-rod" stays at the interface. Looking for a dissociation mechanism for the 1/2[100] dislocation, analogous to that for the Py1 interface, one could arrive at $1/2[100] \rightarrow 1/6[111] + 1/6[2\bar{1}\bar{1}]$ in which a Shockley partial dislocation has been forced to appear.

To check if this representation of the interface and the relaxations is valid we performed anisotropic elastic continuum calculations of an array of dissociated dislocations, using the method described in the appendix of [3]. These calculations allow us to address the glide and climb forces on the Shockley partial, the equilibrium separation between stair-rod and Shockley, and the distribution of the Burgers vector over the Ag and ZnO. So far we have carried out calculations on the basal plane interface of the precipitate with OR3. To simplify matters and concentrate on the dissociation we disregard misfit along $\langle 110 \rangle$. We note that an approximation of ZnO by an infinitely stiff medium would not be justified in this case. Calculation of the distribution of the $1/3\langle 111 \rangle$ Burgers vector shows that 57% is accommodated in Ag and 43% in ZnO. This rather even distribution is mainly an effect of the relatively small difference between the shear moduli of Ag and ZnO. The latter is rather low for a ceramic.

For a similar, hypothetical, interface between Cu and ZnO a remarkable fact would occur. In this case only 48% of the Burgers vector would be accommodated in the metal, and 52% in ZnO. For this dissociation, and the equilibrium separation between the resulting partials, three interactions are of importance. There is a repulsive elastic interaction between the stair-rod and the Shockley, whereas the stacking fault energy leads to an attractive term. The interaction between the Shockley and its image in the ZnO can be either repulsive or attractive, depending on material constants. For the interface between Ag and ZnO this particular interaction is repulsive, and we find an equilibrium separation of 3.5 nm along the glide plane. Dissociation of the Frank partials is therefore a possibility at that interface. At a similar Cu–ZnO interface the Shockley will be attracted to the interface by its image in the ZnO. This, and the fact that the stacking fault energy is higher, causes the equilibrium separation near that interface to be only 1.25 nm. Moreover, the attractive force pulls the Shockley to the interface and is largest close to the interface. It is therefore doubtful that the Shockley will reach the equilibrium separation. In the experiment we find a smaller separation than the 3.5 nm calculated. This is not unexpected, it only points out the fact that we have assumed Volterra-type dislocations to be present whereas the interaction across the interface may be insufficient to lead to that degree of localization. We conclude from these calculations that the dissociation of partial dislocations is a reasonable picture for the relaxations near the Ag-ZnO interfaces. The difference in behaviour of Ag and Cu with regard to dissociation is something we hope to be able to confirm experimentally by comparing the results of our experiments on Ag-ZnO and Cu-ZnO.

Some aspects require further clarification, most notably the significant difference between the structure of the basal plane interfaces of OR2 and OR3. The large difference in separation between the Shockley and stair-rod at these interfaces is likely to be related to the spacing of the array. This system may therefore provide an excellent experimental opportunity to study the interplay between misfit and bond strength: the dislocation content of an interface (or rather the misfit) can be varied in an experiment while keeping the bonding at the interface constant. Moreover, this leads to measurable differences in the core structure. Further experimental and theoretical work is under way to investigate this aspect.

6. SUMMARY

An Ag-Zn alloy was internally oxidized. Precipitates of ZnO with the wurtzite and sphalerite structure were formed. The wurtzite precipitates show predominantly one orientation relation with the Ag matrix: $\{0002\}//\{111\}$ and $\langle 2\bar{1}\bar{1}0 \rangle//\langle 110 \rangle$. These precipitates are platelike and are surrounded by basal plane, first-order prismatic and first-order pyramidal facets. Three other ORs were found, showing a slight tilt around $[2\bar{1}\bar{1}0]$ and sharing some of the facets. On all precipitates, "tilted" interfaces were present, low index ZnO facets almost parallel to low index Ag planes. The geometry on the metal side for most of these interfaces can be represented by an array of partial dislocations. Anisotropic elastic continuum calculations have shown that the relaxations near the interface may be interpreted in terms of a dissociation of the Frank partial dislocations near the interface. These interfaces may provide an

experimental tool to study the effects of interface dislocation density (misfit) on the localization of misfit dislocation cores.

Acknowledgements—The work described in this paper is part of the research program of the Foundation for Fundamental Research on Matter (FOM-Utrecht) and has been made possible by financial support from the Netherlands Foundation for Technical Sciences (STW-Utrecht).

REFERENCES

1. F. Ernst, *Mat. Sci. Eng.* **R14,** 97 (1995).
2. V. Vitek, G. Gutekunst, J. Mayer and M. Rűhle, *Phil. Mag. A* **71,** 1219 (1995).
3. W. P. Vellinga, J. Th. M. De Hosson and V. Vitek, *Acta Mat.* in press.
4. W. P. Vellinga and J. Th. M. De Hosson, *Phil. Mag.*, in press.
5. M. Backhaus-Ricoult, S. Hagège, A. Peyrot and P. J. Moreau, *J. Am. Ceram. Soc.* **77,** 423 (1994).
6. G. Y. Wang and J. Th. M. De Hosson, EUREM (1996).
7. X. Y. Huang, W. Mader and R. Kirchheim, *Acta metall. mater.* **39,** 893 (1991).
8. H. Ichinose, H. Ishii, T. Ichimori and Y. Ishida, *Proc. of ICEM 13-Paris* **2A,** 279, Les Editions de Physique des Ulis, France (1994).
9. J. L. Meijering, *Advances in Materials Research* (edited by H. Herman) Wiley, New York (1971).
10. W. P. Vellinga and J. Th. M. De Hosson, submitted *Phil. Mag. A.*
11. JCPDS 36-1451.
12. S. C. Abrahams and J. L. Bernstein, *Acta. Cryst. B* **25,** 1233 (1969).
13. T. M. Sabine and S. Hogg, *Acta Cryst. B* **25,** 2254 (1969).
14. E. H. Kisi and M. M. Elcombe, *Acta. Cryst. C* **45,** 1867 (1989).
15. *Structure Reports* **27,** 475.
16. J. E. Jaffe and A. C. Hess, *Phys. Rev. B* **48,** 7903 (1993).
17. W. L. Bragg and J. A. Darbyshire, *Trans. Faraday Soc.* **28,** 522 (1932).
18. O. Radczewski and R. Schicht, *Naturwissenschaften* **56,** 514 (1969).
19. O. Radczewski, *Optik* **31,** 126 (1970).
20. V. E. Henrich and P. A. Cox, *The Surface Science of Metal Oxides*, 394, Cambridge University Press, Cambridge (1994).
21. F. Ernst, P. Pirouz and A. H. Heuer, *Phil. Mag. A* **63,** 259 (1991).
22. O. T. Woo, G. C. Weatherly and B. Ramaswami, *Mater. Sci. Eng.* **12,** 123 (1973).
23. M. Kuwabara and J. C. H. Spence, *J. Mater. Res.* **4,** 972 (1989).
24. F. Ernst, *Mater. Res. Soc. Symp. Proc.* **183,** 49 (1990).
25. B. Kooi and J. Th. M. De Hosson, submitted *Philos. Mag. A.*
26. J. M. Howe and R. Gronsky, *Mat. Res. Soc. Proc.* **62,** 241 (1986).
27. O. A. Kupcis and B. Ramaswami, *Mat. Sci. Eng.* **5,** 43 (1969).
28. J. C. A. Huang, R. R. Du and C. P. Flynn, *Phys. Rev. Lett* **66,** 341 (1991).
29. J. C. A. Huang, R. R. Du and C. P. Flynn, *Phys. Rev. B* **44,** 4060 (1991).
30. J. C. A. Huang and C. P. Flynn, *Phil. Mag. Lett* **64,** 71 (1991).
31. Y. Ikuhara, P. Pirouz, A. H. Heuer, S. Yadavalli and C. P. Flynn, *Phil. Mag. A* **70,** 75 (1994).
32. M. Florjanic, W. Mader, M. Rűhle and M. J. Turwitt, *J. de Physique* **46,** C4-129 (1985).
33. V. S. Kaushik, A. K. Datye, D. L. Kendall, B. Martinez-Tovar and D. R. Myers, *Appl. Phys. Lett.* **52,** 1782 (1988).
34. B. W. Dodson, D. R. Myers, A. K. Datye, V. S. Kaushik, D. L. Kendall and B. Martinez-Tovar, *Phys. Rev. Lett.* **61,** 2681 (1988).
35. C. A. M. Mulder and J. T. Klomp, *J. de Physique* **46,** C4-111 (1985).
36. F.-S. Shieu and S. L. Sass, *Acta metall. mater.* **38,** 1653 (1990).
37. K. L. Merkle and B. Shao, *Mat. Res. Soc. Symp. Proc.* **122,** 69 (1988).
38. F. Cosandey and P. Lu, *ICEM 13-Paris* **2A,** 275, *J. de Physique* (1994).
39. F. Cosandey and P. Lu, *Acta metall. mater.* **42,** 1913 (1994).
40. D. G. Brandon, B. Ralph, S. Ranganathan and M. S. Wald, *Acta metall.* **12,** 813 (1964).
41. H. J. Fecht and H. Gleiter, *Acta metall.* **33,** 557 (1987).
42. A. P. Sutton and R. W. Baluffi, *Acta metall.* **35,** 2177 (1987).
43. J. R. Willis, S. C. Jain and R. Bullough, *Philos. Mag.* **64,** 629 (1991).